

# A LATERAL SENSOR FOR THE ALIGNMENT OF TWO FORMATION-FLYING SATELLITES

S. Roose<sup>(1)</sup>, Y. Stockman<sup>(1)</sup>, Z. Sodnik<sup>(2)</sup>

<sup>(1)</sup> Centre Spatial de Liège, Avenue du Pré-Aily, B-4031 Angleur-Liège, Belgium  
+32 4 3824600, sroose@ulg.ac.be

<sup>(2)</sup> European Space Agency - ESA/ESTEC  
Keplerlaan 1, 2201 AZ Noordwijk ZH, The Netherlands  
+31 71 565 5733, Zoran.Sodnik@esa.int

**Abstract:** The coarse lateral sensor is a system able to measure the lateral position between two satellites. It bridges the gap between the alignment accuracy achieved with the radio frequency metrology, and the alignment accuracy required the high-precision optical metrology (fine-lateral and longitudinal sensor). The coarse lateral sensor developed at Centre Spatial de Liège (CSL) is a standalone unit. Once connected to an unregulated 28V power-supply, it delivers, the lateral position of a corner cube retro-reflector (within an angle of 10 arcdeg and from 25 to 250 m) and tracks this position at a rate of 10 Hz. The system is operational with the sun in its field-of-view. Real time centroidisation algorithms allow tracking the image position and feed the on-board computer with this information via a RS422 link, allowing further position stabilization. The coarse lateral sensor has successfully undergone thermal qualification (40°C and -30 °C), and vibration test (high-level sinus, random and shock test in the 3-axis).

**Keywords:** Formation flying, Metrology, Camera.

## 1 Introduction-PROBA-3

The development of this sensor is carried out in the framework of ESA's PROBA-3 mission, which is dedicated to the demonstration of Formation Flying (FF) technologies for future European scientific and application missions. The success of the envisaged missions depends on understanding and correctly implementing all the aspects of FF.

The primary mission objective for PROBA-3 is to demonstrate FF through [1] [2]:

- Flight qualification of FF hardware, which currently are foreseen to be:
- Extrapolated GPS metrology
- Optical metrology
- High accuracy propulsion system
- FF Guidance, Navigation and Control (GNC) system
- Demonstration of FF manoeuvres for future missions
- Exploitation of the FF for scientific return

The PROBA-3 embarks a scientific mission which is a sun coronagraph. On the satellite 1 (here the coronagraph) a camera and an imaging system looks at the sun which is obscured by a second satellite 2 (the occulter) (Figure 1).

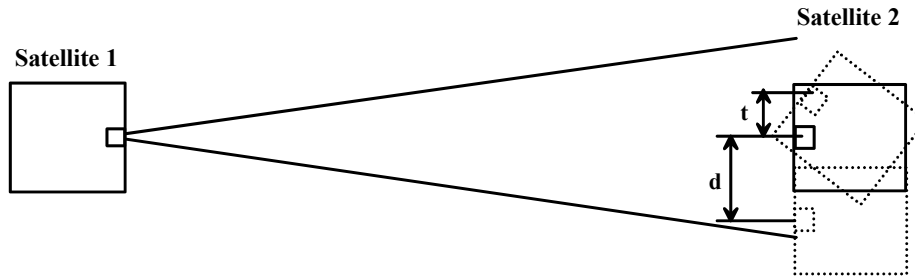


**Figure 1. Coarse lateral displacement in formation flying.**

The second satellite 2 has at least one co-operative target like a corner cube retro-reflector. A laser source will be mounted on satellite 1. This source is aligned with the imaging system.

If one assumes that only lateral translation “d” needs to be recorded, a single target is sufficient. Unfortunately, the relative rigid body motion of a spacecraft can show also a translation “t” of the target due to rotation.

In the current specification, attitude of the S/C will be controlled within  $\pm 10$  arcsec. It is understood that the S/C will face toward each other with this accuracy. Given the typical dimensions of the PROBA 3 S/C (1 m) we can say that with this accuracy the position of a target will be controlled within a volume of  $100 \mu\text{m}$  size ( $t < 100 \mu\text{m}$ ). This is negligible with respect to the millimeter accuracy level, requested for the CLS in this work.

An earlier article describes the optical design and metrology performances [3]. A full system and qualification test are described here.

## **2 Architecture**

The lateral sensor developed at Centre Spatial de Liège is based on a camera (CMOS detector: Cypress HAS2 CMOS APS type detector [4]. that allows quick read-out of sub-windows of interest), a telecentric lens designed at CSL, a fibre-coupled laser-diode bar and a corner cube.

The fibre-coupled laser-diode bar emits a diverging beam, from the master spacecraft to the slave spacecraft. A corner cube located on the slave spacecraft sends the light back. This light is captured by the telecentric lens and camera (built by Deltatec Liège-B). A lateral shift “d” of the corner cube is seen on the camera as an image displacement. Real time centroidisation algorithms will allow tracking the image position and feed the on-board computer with this information via a RS422 link, allowing further position stabilisation. The imaging system is adjusted and designed for a depth of field from 25 m to 250 m.

The CLS is based on the following architecture (Figure 2):

- A corner cube (50 mm - diameter) which is the target on the Occulter S/C.
- A CLS telescope unit containing a barrel, lens(es), Interference filter, neutral Density Filter, Alignment Cube. The CLS telescope unit is composed of 5 lenses, 2 filters, an alignment cube and a divergent lens.
- A CLS detector unit based on a Cypress HAS2 CMOS APS detector [2].
- The centroid data is downloaded via a RS422 link to an EGSE (Electrical ground support equipment).
- The laser diode driver is controller via the detector unit.
- The laser diode itself is a fiber optic pump laser diode (Instantaneous Optical Power 40 W) attached to a fiber collimator/NA converter.

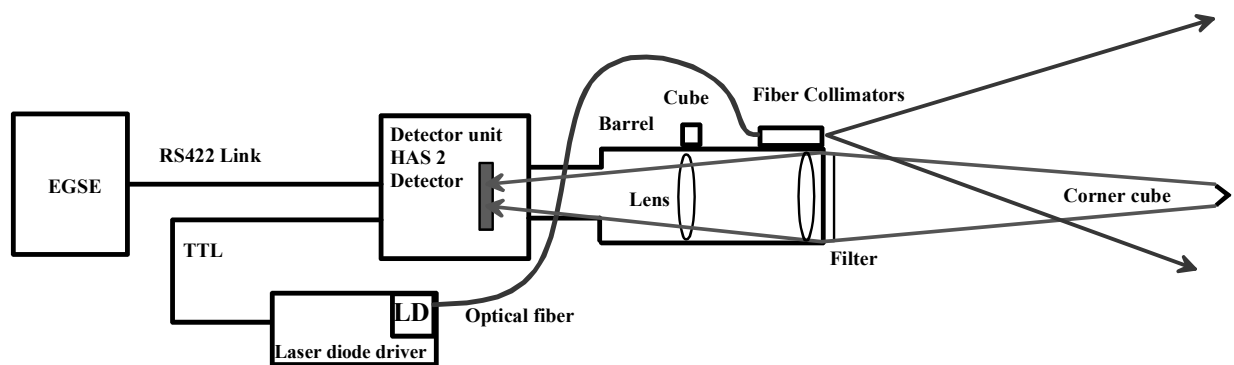


**Figure 2. Architecture of the Coarse Lateral Sensor. The measured data is send to the EGSE (Electrical Ground Support equipment).**

Because of the large depth of operation, all lateral system performances are angular ones. The system requires:

Tracking capability for a spot moving @ 0.5 arcdeg/sec in the field of view of the camera.

Spot detection with the sun (bright source) in the field of view.

Centroidisation accuracy: 0.1 camera pixels (3.5 arcsec).

Absolute calibration accuracy: 0.14 camera pixels (5 arcsec).

In order to comply with these requirements, the following features were implemented:

- The camera allows quick read-out of sub-windows of interest (in 1 ms).
- Optimize radiometric budget and laser diode power consumption, and its related heat dissipation.
- An interference filter blocks all unwanted light centred on the laser wavelength (980 nm).
- Implementation of a “slow detection mode”, which allows to discriminate sun from moving image.

The system is a standalone unit. Once connected to an unregulated 28V power-supply, it delivers, after spot detection, pixel coordinates to the RS422 link at a 10 Hz rate. Its average power consumption is less than 8W.

The system can be put in a programming mode, to allow uploading settings in the camera.

Tracking, absolute calibration, resolution and sun avoidance have been measured in a field of 10 arcdeg and the range of depth of 5 m to 80 m.

The coarse lateral sensor has successfully undergone thermal qualification (40°C and -30 °C), and vibration test (high-level sinus, random and shock test in the 3-axis). Its metrology performances (centroidisation accuracy (<0.1 pixel RMS) and tracking) remained unchanged after these qualification tests. The absolute calibration is 0.3% in the interval of  $\pm 5$ arcdeg (11 arcsec in  $\pm 1$ arcdeg).

### 3 Optical Design

The system operates as an angle to position converter. The angular accuracy requirement is 5 arcsec in a FOV of 10 arcdeg. The 10 arcdeg are imaged on a 1024 x 1024 HAS detector (18  $\mu$ m pixel).

The system is telecentric in the image plane (Figure 3). The Neutral Density Filter (NDF) and interference filter (IF) are placed as first components. Putting the NDF as first lens will act as a cold filter and by this way reduces the thermal load on the CLS.

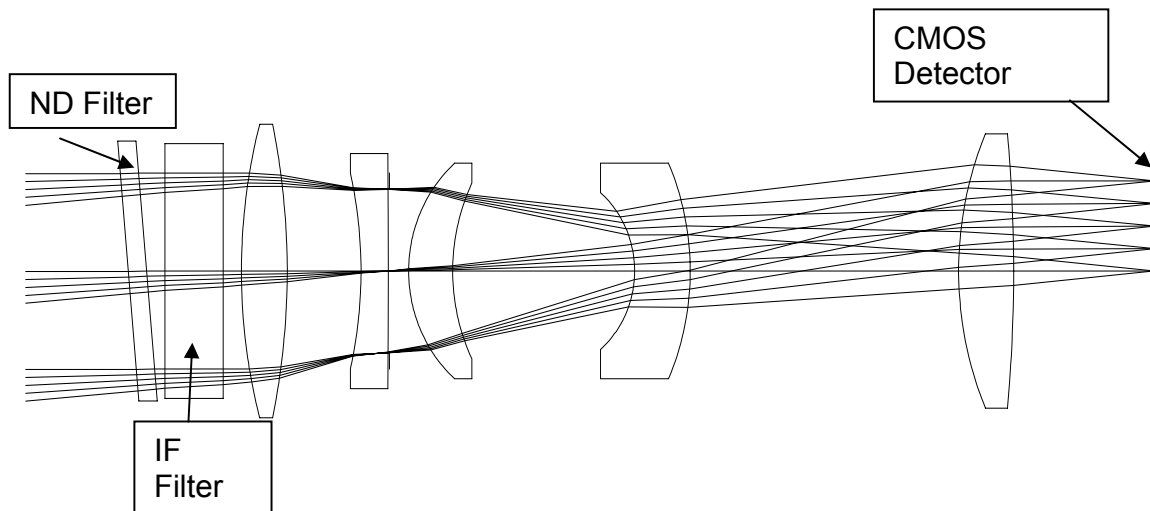


Figure 3. Schematics of the CLS telescope lens design.

One interference filter blocks unwanted light out of the band of 980 nm  $\pm$  5nm. The mechanical concept is shown in Figure 4. The lenses are contained in a lens barrel. One fibre collimators is also shown on the drawing, and one alignment cube. The weight is 418 g, considering all the mechanical part in Aluminum.

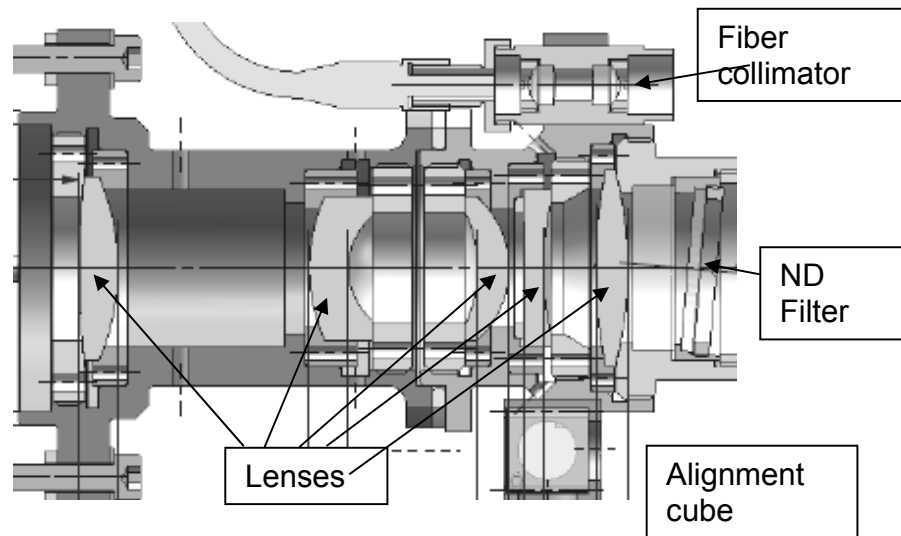


Figure 4. Lens barrel mechanical design.

## 4 Detector Design Unit

### 4.1 Architecture

The CLS detector unit consists of:

- HAS CMOS APS image sensor from Cypress.
- Proximity detector electronics, clock drivers, control, signal conditioning.
- On-board processor based processing for centroid computation.
- A bi-directional RS422 serial link for centroid coordinates/status read-out and CLS control.
- A high speed unidirectional serial link for EGSE image read-out and data read-out.

The CLS serial link supports the following functions:

- Setting of the CLS functional parameters
- Reading the centroid coordinates
- Setting the CLS functional mode
- Reading the CLS status
- Test related commands

The on-board camera processor will find for every frame (max 10 Hz) the centroid (X, Y coordinates) of corresponding corner-cube image.

The on-board camera processor controls the laser diode on/off switch through a TTL output (automatic command to switch-on/off the laser diode during acquisition).

## 4.2 Electronics

The electronic board is built using a flex PCB comprising three multilayer rigid sections bound by two double layer flex sections (Figure 5).

- A sensor PCB contains the HAS sensor and several passive components used for decoupling and biasing the chip.
- A digitalisation section which provides the signal conditioning and the Analog to Digital conversion.
- A digital section that is busy with the processing and the communication with the on-board computer, power supply and accessories.

The next picture shows the whole electronic board bent as it should be to fit within the detector enclosure, without all its fixing accessories.

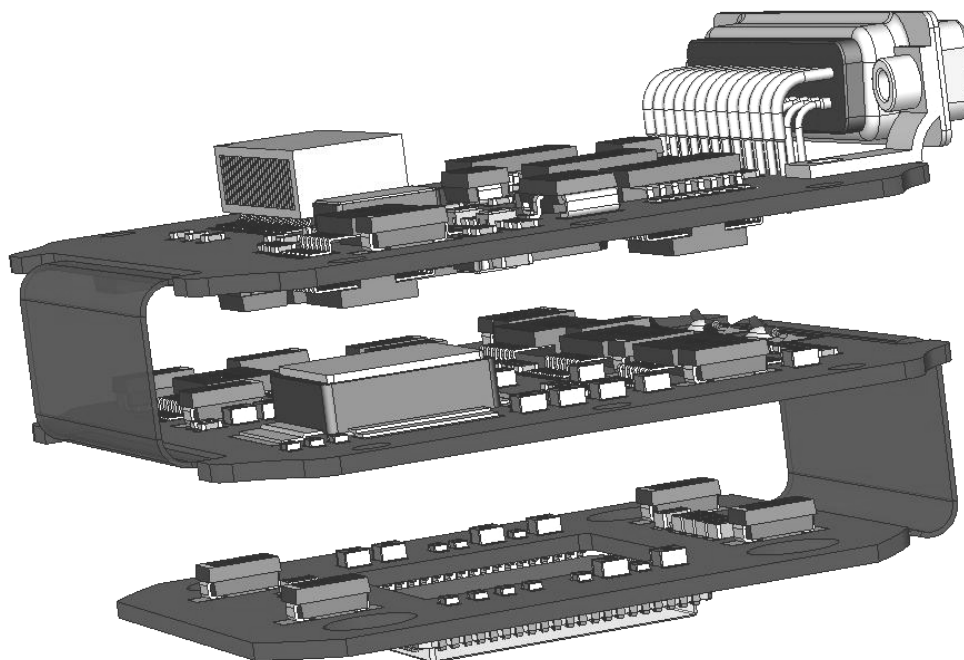


Figure 5. Bent flex PCB assembly

## 4.3 Algorithm

The CLS has as main function to detect, identify, track and measure the position of the image of the corner cube on the detector.

During the acquisition mode, the detector is scanned in stripes of 16 lines (Figure 5). The capture time  $10 \text{ MHz} \times 1024 \text{ pixels} \times 16 \text{ lines} + 1 \text{ ms} = 2.6 \text{ ms}$ . The slew rate of the images is maximum  $0.5 \text{ deg/s} \times 102.4 \text{ pixel/deg} \times 1 \text{ ms} = 0.05 \text{ pixel/ms}$ . This corresponds to 0.13 pixel.

The system will make a stripe image with laser diode ON and OFF. All quasi static images (light distributions) will give a zero output. If the image of the corner cube appears in these stripes it will give an acceptable “i” “j” coordinate that will be transferred to the tracking mode.

The major steps in the tracking algorithm are (Figure 6):

- Take a reference image (the laser diode is turned off) on the tracking window.
- Take the spot image in the same conditions (the laser diode is turned on).
- Compute the difference between the spot image and the reference image (this will result in a “processed image” where pixel values can be negative).
- Compute the Center Of Gravity (COG) values on this processed image.
- Compute centroid offset with previous acquisition and move the tracking window
- Send the image coordinates to the spacecraft

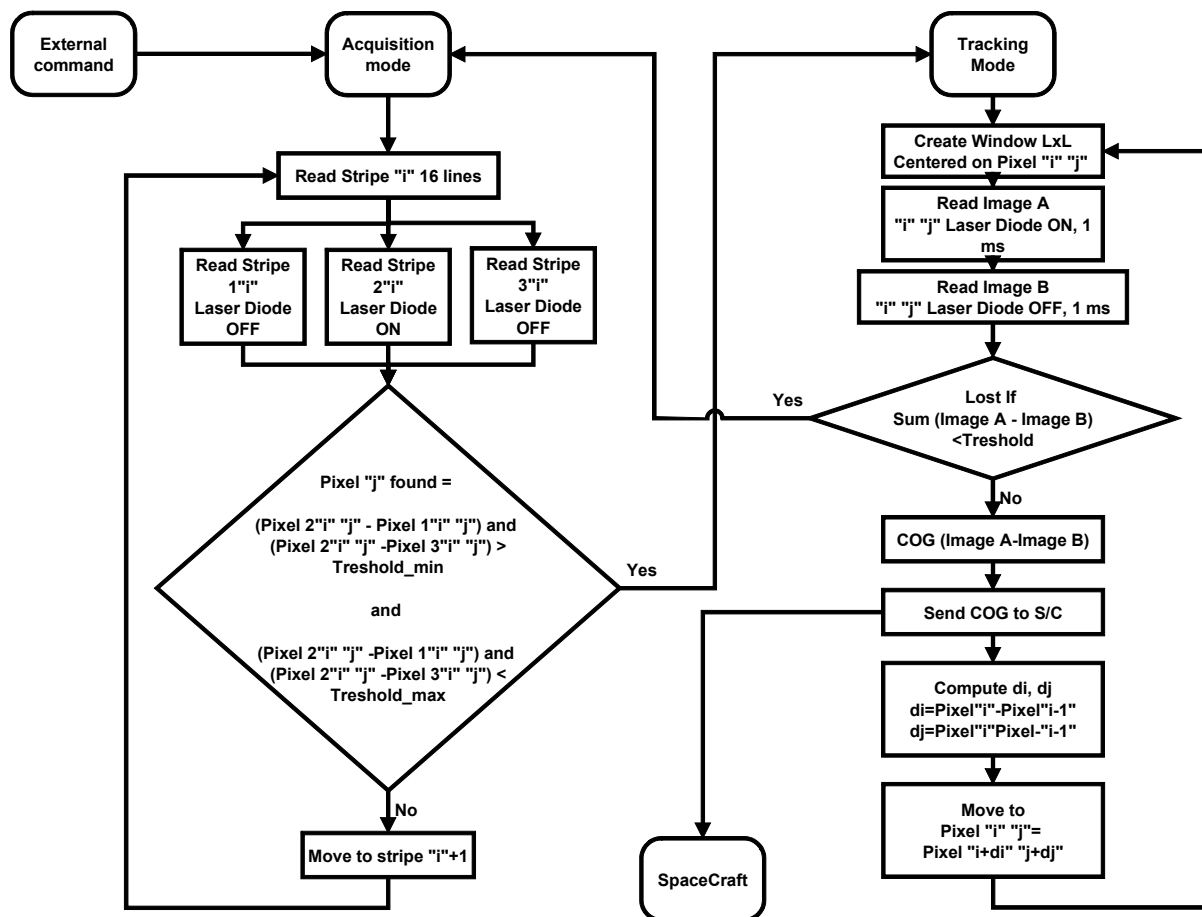


Figure 6. Acquisition and Tracking flow chart.

#### 4.4 Detector unit housing

The detector unit (camera and lens barrel) are fixed together to form the complete CLS device as can be seen on the following picture. The device is attached on the platform using an additional corner plate, or by the rear side of the detector unit.

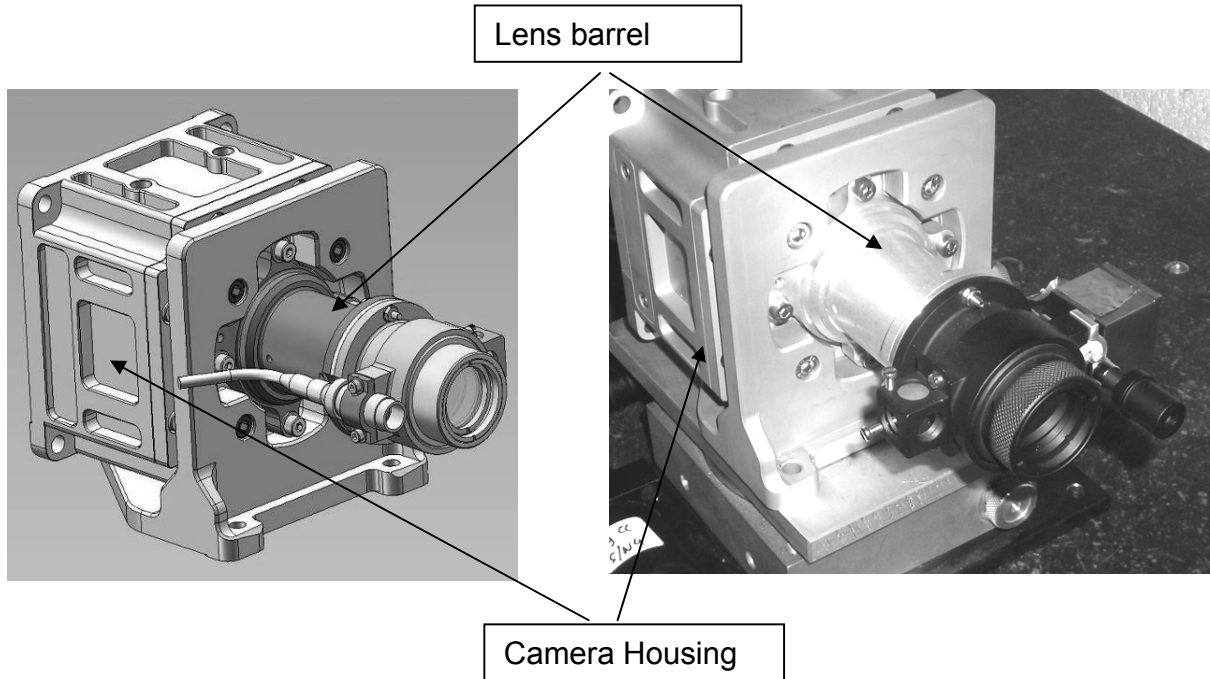


Figure 7. CLS Detector Unit- Overall view.

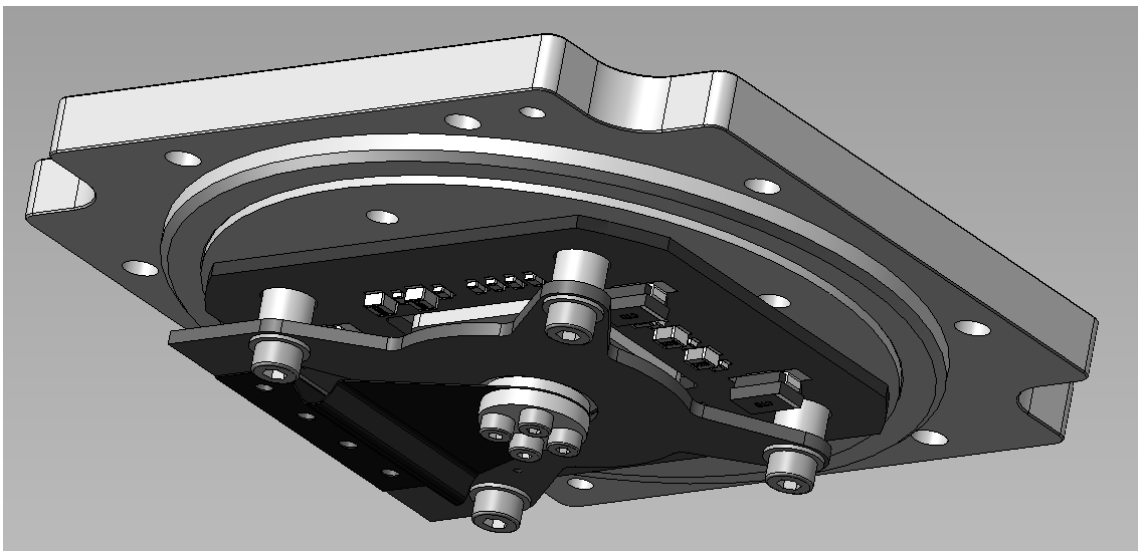


Figure 8. Sensor unit - Detector is glued on its Titanium interface



The sensor unit is the most critical part of the device since it concentrates most of the accuracy requirements of the CLS. It is mostly built out of the following parts :

The sensor base frame which is circular and very accurately milled (Figure 8). It includes the contact and fixing features for the sensor PCB. The HAS sensor is the key fixed part of this assembly. Its positioning must be very carefully tuned before gluing it on the frame. The front glass is fixed against a small bezel ensuring no tilt around X and Y axis as well as accurate Z positioning. The X and Y offsets and Z-tilt must be kept within acceptable limits by the use of a specifically designed positioning tool while gluing the sensor on the frame.

## 5 Source Unit Design

The Source Unit (SU) contains the power electronics to drive camera and laserdiode: DIODE QD-Q6818-FL4 (18W in CW, 40 W in QCW 400µm Compact Fiber Coupled module @ 980nm).

The Source unit has to provide the following voltages (Figure 9):

Laser-Diode driver: +30V with a capability of 2 Amps peak.

Detector Unit:

- +/-5V with a capability of 100 mA.
- +3.3V with a capability of 1000 mA.

Input voltage will be an unregulated 28V Bus (from xx V to xx V)

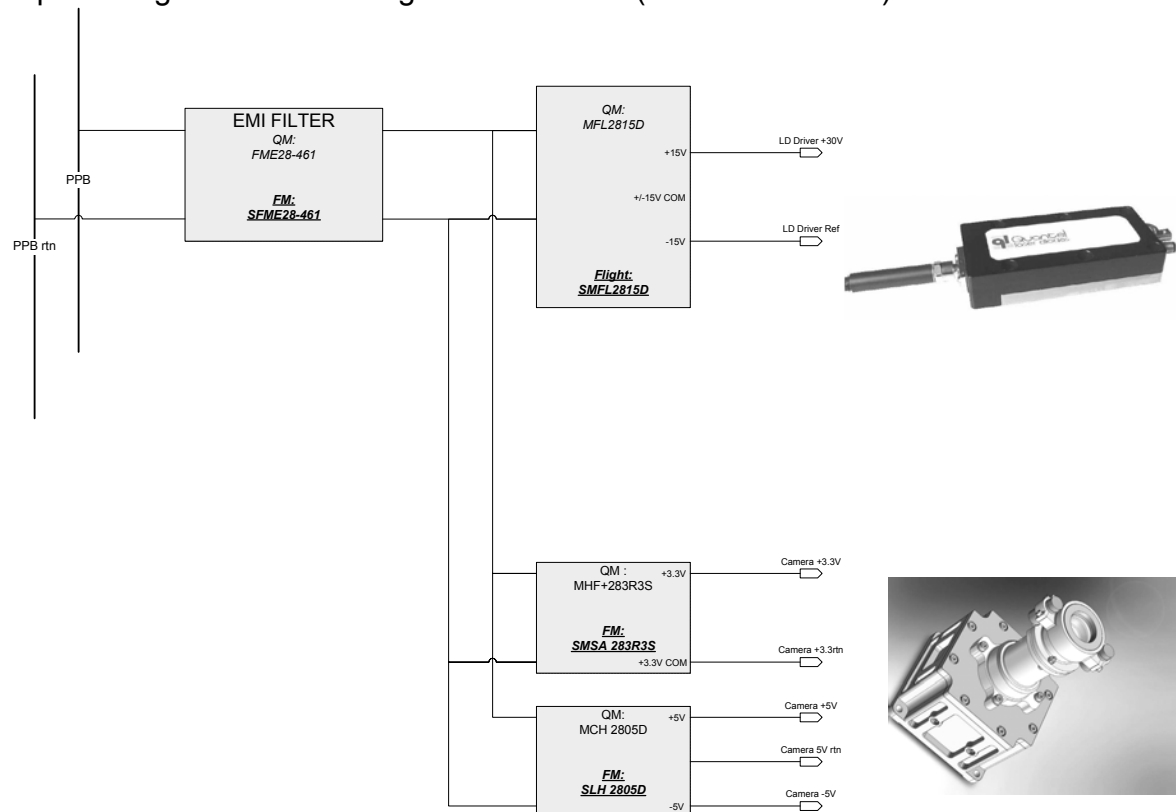
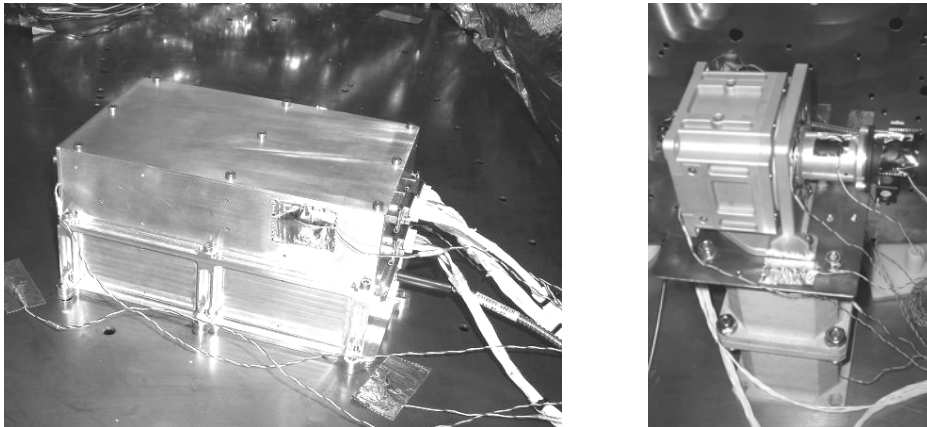


Figure 9. DC-DC overview

## 6 Environmental tests

The electronic box and camera unit were mounted into two separated thermal tents in CSL's FOCAL 5 facility. Both tents were controlled independently in temperature to undergo thermal cycles at a pressure of less than  $1e-5$  mbar.

The electronic box was conductively mounted on the copper panels of its thermal tent, while the detector unit was interfaced to a copper panel which was itself mounted on a low thermal conductive PermaGlass support (Figure 10)..



**Figure 10. (Left) Electronic box mounted in its thermal tent, (Right) Camera mounted on PermaGlass Interface**

This PermaGlass has a low conductivity and isolates the camera from the optical bench. The thermal cycle profiles (328 K to 233 K for the camera/lens/detector unit) are presented in Figure 11.

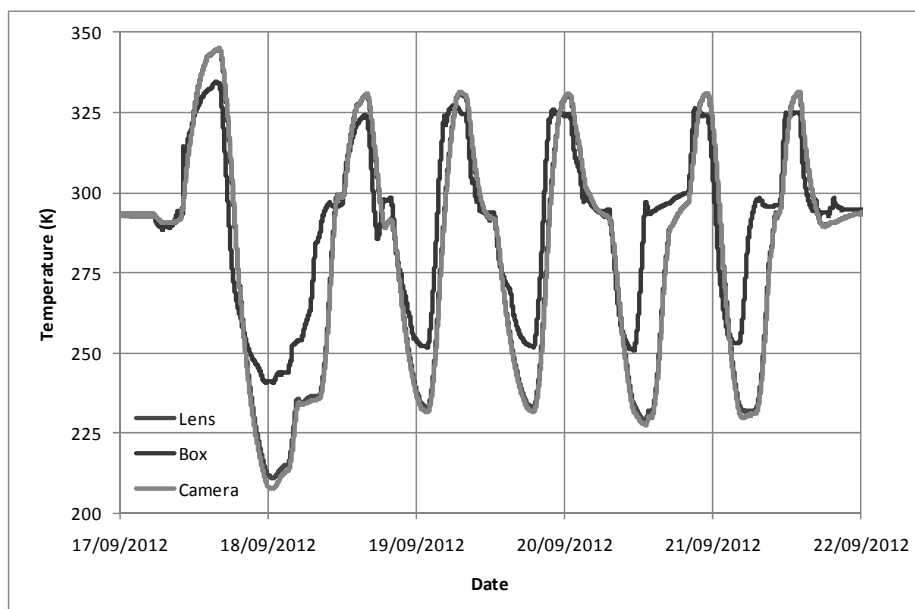


**Figure 11. Thermal vacuum cycle showing average temperature of camera and electronic box.**

The unit was also vibrated along 3 axis (18.4 g RMS random test, 20 g sine test), optical calibrations were performed before and after the environmental test campaign. Low level sine resonance search confirms a first eigen-frequency above 140 Hz: 239 Hz (Figure 13)

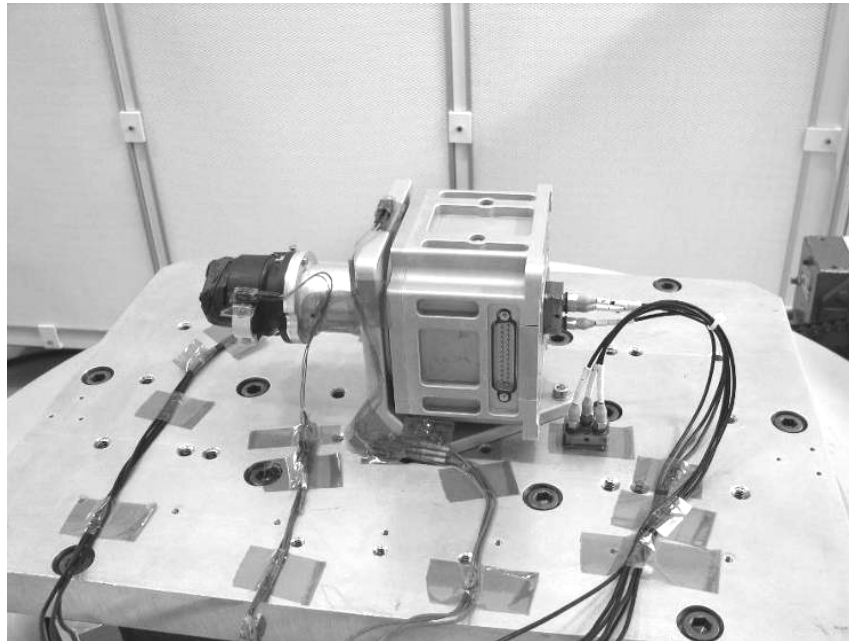


**Figure 12. CLS head on the slip table of a shaker.**

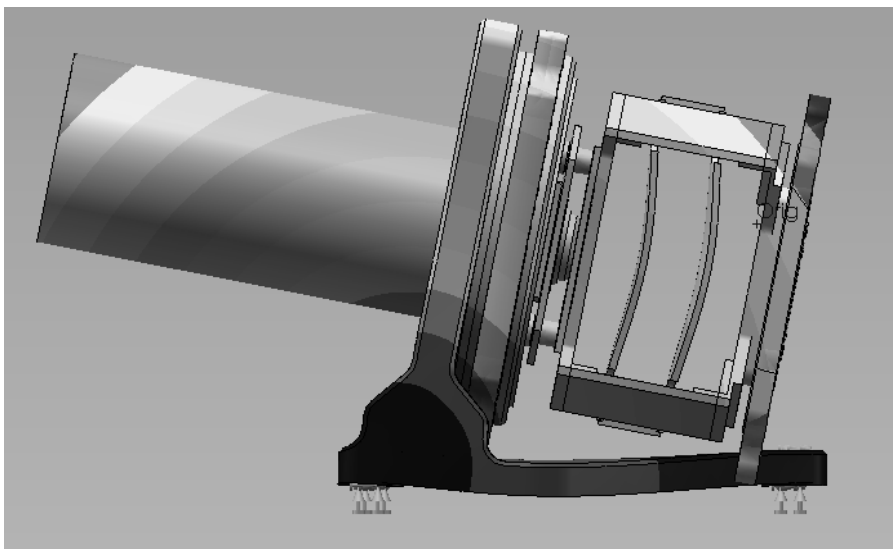


**Figure 13. Main Structure – Mode 1 : 239 Hz**

## 7 Optical performance test

### 7.1 Detection and tracking with the sun in the field of view

This capability has been demonstrated with a sun simulator giving 1/3 of a solar constant as flux.

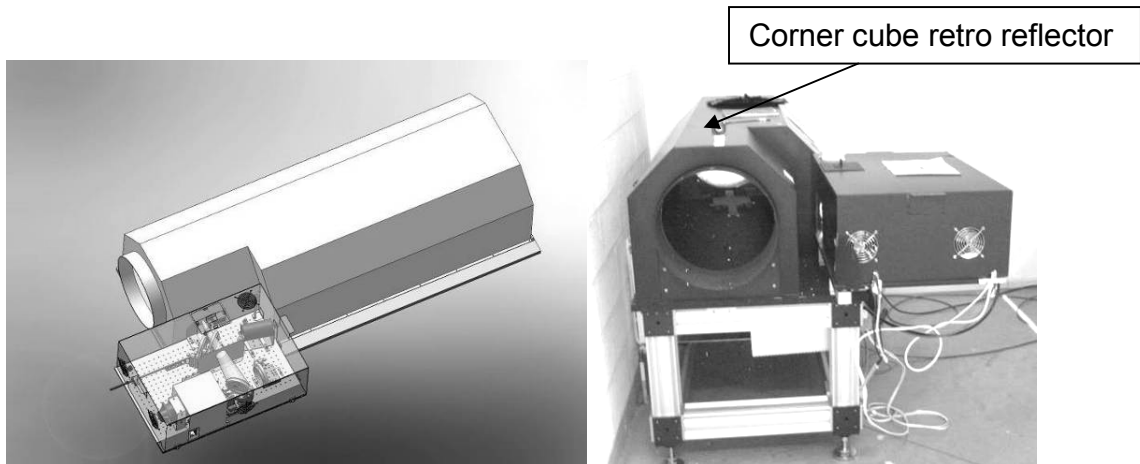


**Figure 14. Sun simulator. The entrance aperture is 380 mm diameter. The corner cube is mounted on top of the sun simulator during this experiment (see right picture).**

Tracking capability verification for a spot moving @ 0.5 arcdeg/sec with spot occultation was also demonstrated in this testing phase.

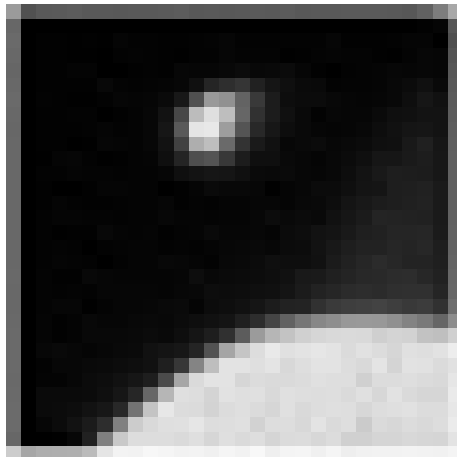


**Figure 15. Image of the corner cube and the beam coming from the sun simulator. Note the projected sun has an equivalent field diameter of 50 pixel. We see a part of the sun in the tracking window. The tracking window is 30 pixels wide. The sun is a static image and is subtracted when taking 2 sequential images of 1 ms (one source on, one source off).**

## 7.2 Tracking and tracking recovery

Tracking capability verification for a spot moving @ 0.5 arcdeg/sec is shown hereunder without and with beam interruption (Figure 16).

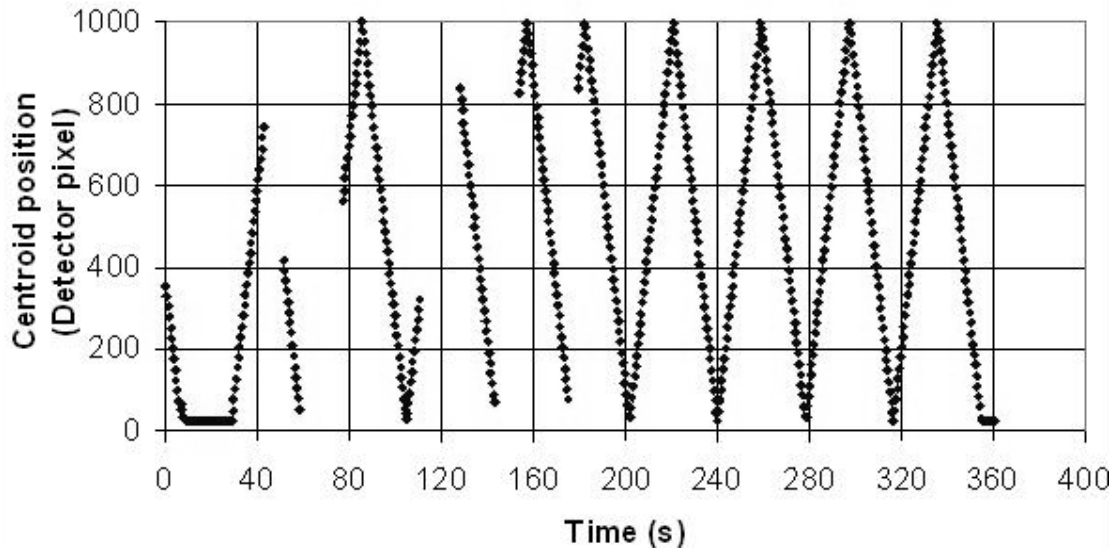


Figure 16. Tracking capability verification for a spot moving @ 0.5 arcdeg/sec with spot interruption. The interrupted curve shows the detection recovery.

## 7.3 Functional test during the thermal cycling test

The system capability was tested during these cycles. However, the measurement distance from camera to corner cube ( $\varnothing 25$  mm) was  $13.2 \text{ m} \pm 0.1 \text{ m}$ .

The stability of the focal length in temperature range is 0.4% of the focal length and a the focal length repeatability between the cycles (for same temperatures) is also 0.4%. This indicates that our measurement uncertainty is driven by the uncertainty of our calibration bench. Repeatability of the optical axis is 0.3 pixels.

## 7.4 System calibration in the working volume

The image position of the corner-cube retro-reflector was recorded on the camera detector for various angular position of the camera with respect to the corner cube. It gives a typical linear curve, with a slope, the focal length of the system.

Interesting is the evolution of the focal length which is characterizes the thermo-elastic behavior of the optics. This measurement was done for various distances (20 m, 40 m, 80 m) and after different tests. The slope of the calibration curve is the focal length of the system. We have analyzed the dispersion of this focal length in the measurement volume. The RMS dispersion on the measurement @40m is 0.28 mm or 0.3% of the focal length.

This is the uncertainty that we achieve on the focal length measurement, and this is the uncertainty on the absolute calibration. This means practically that we have a image scaling uncertainty of 0.3%.

Test conditions	Focal length (mm)
@20m, after TV test	102.77
@40m, after TV test	102.55
@80m, after TV test	102.28
@20m, after vibration test	102.68
@40m, after vibration test	102.67
@80m, after vibration test	102.18

**Table 1. Calibration epochs and evolution of the measured focal length.**

This uncertainty on the focal length is mainly due to an uncertainty in our calibration bench. Indeed the angular encoders of the rotation stage are specified with an 0.23 arcdeg accuracy. For an angle of 5 arcdeg we have 0.46% uncertainty. A specific calibration bench with 1 arcsec position knowledge of the corner cube retro-reflector need to be build in the future.

## 8 Conclusion

The coarse lateral sensor is a stand-alone detection system, which provides automatic coordinates of the image of a corner cube even with the sun in the field of view. The system operates in a narrow band around 980 nm.

The only electrical interface with the spacecraft is a RS422 link and an unregulated spacecraft 28 V power bus.

The coarse lateral sensor has successfully undergone thermal qualification and vibration test. Its metrology performances (centroidisation accuracy (<0.1 pixel RMS) and tracking) remained unchanged after these qualification tests.

The functional test, performance test and stray light test have demonstrated that the CLS head is conform (@1 bar, @293 K) in terms of:

- Position resolution of 3.6 arcsec within the FOV (with the sun in the FOV)
- Acquisition and tracking speed of 0.5 arcdeg/s (with the sun in the FOV)

Operational measurement distance:	Designed for 250 m. Verified in ambient conditions to 84 m. TV tested @13.2 m
Lateral displacement range (in two dimensions):	±5arcdeg In thermal vacuum tested in a range of 0.5 arcdeg
Lateral displacement accuracy (3 Sigma):	Centroidisation accuracy < 3.6 arcsec (13.2 m to 84 m, ±5arcdeg) Absolute calibration known today with an uncertainty of 0.3% in the FOV of ±5arcdeg (11 arcsec in ±1arcdeg)
Maximum lateral range rate:	0.5 arcdeg/sec
Measurement bandwidth:	980 nm
Volume of receiver (200 mm x 100 mm x 100 mm)	But source unit is not considered in this volume
Total mass	1.6 kg DU + 1.6 kg SU cables excluded
Total power consumption	7.85W average
Operational pressure range	1 Bar to 1e-6 mbar
Data interface	RS422
Random test	18.4 g RMS
Sine test	20 g
Shock test	Simulated by half sine test
Thermal environment and test requirements	Cold start up of the detector head demonstrated

Table 2. CLS characteristics.

## 9 ACKNOWLEDGEMENTS

This work was performed under the ESA Belgium GSTP contract 22251/09/NL/NA - Optical Metrology: Coarse Lateral Sensor (CLS).

## 10 REFERENCES

- [1] J. Borde et al., Feasibility of the Proba 3 formation flying demonstration mission as a pair of microsats in GTO, Proceedings of The 4S Symposium: Small Satellites, Systems and Services (ESA SP-571). 20 - 24 September 2004, La Rochelle, France. Editor: B. Warmbein. Published on CDROM., p.12.1 (2004).
- [2] L. Tarabini Castellani et al., "PROBA-3 FORMATION FLYING MISSION", 7<sup>th</sup> International Workshop on Spacecraft Constellation and Formation Flying, Proc. IWSCFF-2013-08-07, Lisbon (2013).
- [3] S. Roose et al. , "A Lateral sensor for the alignment of two formation-flying satellites", "Optical Measurement Systems for Industrial Inspection VIII" Optical metrology 2013, Munich, Proc. SPIE 8788, paper 8788-71(2013).
- [4] CYPRESS, "HAS2 Detailed Specification – ICD", APS2-CY-FOS-06-004, (2009).